

1 **Whole-genome resequencing data support a single introduction of**
2 **the invasive white pine sawfly, *Diprion similis***

3
4 Jeremy S. Davis^{1*}, Sheina Sim², Scott Geib², Brian Sheffler³, Catherine R. Linnen¹

5
6 ¹Dept. of Biology, University of Kentucky, Lexington, KY, 40508

7 ²USDA-ARS, Daniel Inouye Pacific Basin Agricultural Research Center, Hilo, HI, 96720

8 ³USDA-ARS, Jamie Whitten Delta States Research Center, Stoneville, MS, 38776

9 *Corresponding author: j.davis@uky.edu

10

11 **Running title:** Population structure of an invasive pine sawfly

12 **Abstract**

13 Biological introductions are unintended “natural experiments” that provide unique insights into
14 evolutionary processes. Invasive phytophagous insects are of particular interest to evolutionary
15 biologists studying adaptation, as introductions often require rapid adaptation to novel host
16 plants. However, adaptive potential of invasive populations may be limited by reduced genetic
17 diversity—a problem known as the “genetic paradox of invasions”. One potential solution to this
18 paradox is if there are multiple invasive waves that bolster genetic variation in invasive
19 populations. Evaluating this hypothesis requires characterizing genetic variation and population
20 structure in the introduced range. To this end, we assemble a reference genome and describe
21 patterns of genetic variation in the introduced white pine sawfly, *Diprion similis*. This species
22 was introduced to North America in 1914, where it has undergone a rapid host shift to the thin-
23 needled eastern white pine (*Pinus strobus*), making it an ideal invasion system for studying
24 adaptation to novel environments. To evaluate evidence of multiple introductions, we generated
25 whole-genome resequencing data for 64 *D. similis* females sampled across the North American
26 range. Both model-based and model-free clustering analyses supported a single population for
27 North American *D. similis*. Within this population, we found evidence of isolation-by-distance
28 and a pattern of declining heterozygosity with distance from the hypothesized introduction site.
29 Together, these results support a single-introduction event. We consider implications of these
30 findings for the genetic paradox of invasion and discuss priorities for future research in *D.*
31 *similis*, a promising model system for invasion biology.

32

33 **Keywords:** invasion biology, population structure, adaptation, non-model genome,
34 *Hymenoptera*, phytophagous insect

35 **Introduction**

36 Human-mediated biological introductions are a ubiquitous part of changing global
37 ecosystems with negative consequences for local flora and fauna (Carlton and Geller 1993,
38 Wonham et al. 2001, Simberloff 2013, Capinha et al. 2015). Biological introductions involving
39 plant-feeding (phytophagous) insects are particularly common and can cause widespread damage
40 to local crops and plants (Schulz et al. 2020, Lesieur et al. 2019). This destruction is exacerbated
41 when insects adapt to native plant hosts, which can lead to rapid range expansion and added
42 complications for controlling the invasion (Kennedy and Storer 2000). For this reason,
43 understanding how and why host shifts occur in invasive species is of considerable applied
44 importance (Clavero and Garcia-Berthou 2005, Oerke 2005). From a basic research perspective,
45 invasive species are unintentional “evolutionary experiments” that enable us to better understand
46 the genetic and evolutionary mechanisms underlying rapid host adaptation (North et al. 2021,
47 Forister et al. 2012, Futuyma and Moreno 1988, Lee 2002, Vertacnik and Linnen 2017, Prentis et
48 al. 2008). Despite considerable research effort (Bock et al. 2015, North et al. 2021) many
49 questions regarding evolution in invasive populations remain unresolved.

50 One unresolved question in invasion biology asks: Given the profound reduction in
51 genetic variation that accompanies many species introductions, how do invading populations
52 have sufficient raw genetic material to adapt to novel environments (Allendorf & Lundquist
53 2003, Frankham 2005)? In recent years, the prevalence of this so-called ‘invasion paradox’ has
54 been challenged (Estoup et al. 2016, Dlugosch and Parker 2008), with several studies failing to
55 find evidence of reduced diversity in recently introduced populations (Roman and Darling 2007,
56 Facon et al. 2008, Kolbe et al. 2004—but see Kanuch et al. 2021). A common mechanism for
57 maintaining high levels of genetic variation in invasive populations is admixture between

58 multiple genetically distinct invading populations (Bock et al. 2015, Dlugosch and Parker 2008,
59 Prentis et al. 2008, Rius and Darling 2014). Most evidence used to support a multiple-invasion
60 scenario is the existence of multiple genetically distinct groups within the introduced range, often
61 inferred via patterns of population structure (Jaspers et al. 2021, Fitzpatrick et al. 2012, Sherpa et
62 al. 2019). However, population structure can be missed when too few individuals or genetic
63 markers are sampled (Sherpa et al. 2018, Lewald 2021). To reconstruct the demographic history
64 of invasions and identify recent targets of selection, genome-scale data (e.g., whole-genome re-
65 sequencing (WGS) data, are ideal (North et al. 2021). Analysis of WGS data is greatly facilitated
66 by high quality reference genomes; however, genomic resources are still lacking for many
67 insects (Hotaling et al. 2021, North et al. 2021, Ekblom and Galindo 2011).

68 Here, we develop genomic resources and describe population structure for invasive
69 populations of *Diprion similis* (Hymenoptera: Diprionidae), a potentially powerful model for
70 invasion population genomics. *D. similis* is an ideal organism for studying adaptation following
71 invasion: it has undergone a pronounced host shift in the invasive range, and the introduction and
72 spread of this species is well documented in literature and museum collections (Britton 1915,
73 Britton 1916, Middleton 1923). *D. similis* was first recorded in Connecticut, 1914 and rapidly
74 spread across eastern North. In its native Eurasian range, *D. similis* is found primarily on the
75 thick and resinous needled Scots pine, *Pinus sylvestris*. In North America, however, *D. similis* is
76 mostly found on a native, thin-needled pine, eastern white pine (*Pinus strobus*) (Lyons 2014,
77 Coppel et al. 1974). This host association is common enough that North American *D. similis* is
78 now casually referred to as the “introduced white-pine sawfly” by the research community. The
79 shift from a thick-needled Eurasian host to a strikingly thin-needled North American host is
80 somewhat surprising because thin needles represent a substantial ecological barrier to successful

81 reproduction in many diprionids. This is because sawfly females must embed their eggs within
82 needles without cutting too deeply, or eggs will fail to develop (Figure 1B; Knerer and Atwood
83 1973, McCullough and Wagner 1993, Codella and Raffa 2002, Bendall et al. 2017). Indeed,
84 although white pine is widespread and abundant in eastern North America, only a single native
85 diprionid, *Neodiprion pinetum*, uses this host regularly (Linnen and Farrell 2010). *N. pinetum* has
86 also evolved several adaptations for laying eggs in thin needles, including smaller eggs, smaller
87 ovipositors, and a unique egg-laying pattern (Bendall et al. 2017, Bendall et al. 2022, Glover et
88 al. in prep).

89 As a first step to understanding how invasive *D. similis* populations were able to adapt to
90 a novel and particularly challenging host, we describe patterns of population structure in the
91 invasive range. To do so, we assemble a high-quality reference genome for this species, to which
92 we map low-coverage whole-genome sequence data from 64 diploid *D. similis* individuals
93 sampled across eastern North America. With these data, we examined three spatial patterns of
94 genetic variation to evaluate support for single-invasion vs. multiple-invasion scenarios. First, a
95 single introduction is expected to yield a single genetic cluster within the introduced range, while
96 multiple invasions would be detectable as genetically distinct groups (van Boheeman et al. 2017,
97 Sherpa et al. 2019). Second, in a single-introduction scenario—and assuming sufficient time for
98 invasive populations to reach drift-migration equilibrium—genetic distance between individuals
99 in the introduced range is expected to follow a mostly continuous pattern of isolation-by-
100 distance, whereas discontinuities in the spatial distribution of genetic variation would be
101 indicative of multiple recent invasions (Sherpa et al. 2018). Third, under a single-invasion
102 scenario, genetic diversity should decrease from the point of introduction due to repeated founder
103 effects and consistently smaller population sizes on the edge of range expansion; by contrast, a

104 multiple-invasion scenario with multiple points of introduction would increase diversity and
105 disrupt spatial patterns of genetic diversity (Van Petegem et al. 2017, Biolozyt et al. 2005,
106 Hewitt 1993). By evaluating our data considering these predictions, we conclude that sampled
107 North American populations of *D. similis* most likely came from a single invasion. In the
108 discussion, we consider limitations of our data and explanations for how these populations were
109 able to adapt to novel hosts in the absence of an influx of genetic variation via admixture.

110

111 **Materials and Methods**

112 *DNA extraction and library preparation*

113 For assembling a reference genome, genomic DNA from *D. similis* was isolated from one
114 haploid male eonymph that was flash frozen in liquid nitrogen. Genomic nucleic acid isolation
115 was performed using the MagAttract HMW DNA Kit (Qiagen, Hilden Germany) precisely
116 following the instructions of the fresh or frozen tissue protocol. After isolation, a 2.0x Solid
117 Phase Reverse Immobilisation (SPRI) bead clean-up was performed to improve sample purity.
118 At each step, double-stranded DNA was quantified using the dsDNA Broad Range (BR) Qubit
119 assay and the fluorometer feature of a DS-11 Spectrophotometer and Fluorometer (DeNovix Inc,
120 Wilmington, DE, USA). Sample purity was determined with the UV-Vis spectrometer feature on
121 the DS-11 which reported OD 260/230 and 260/280 ratios. Isolated genomic DNA was sheared
122 to a mean size distribution of 20 kb using a Diagenode Megaruptor 2 (Denville, New Jersey,
123 USA) and fragment size was confirmed using a Fragment Analyzer (Agilent Technologies, Santa
124 Clara, California, USA) using the High Sensitivity (HS) Large Fragment kit. The sheared DNA
125 was used for PacBio SMRTBell library preparation using the SMRTbell Express Template Prep
126 Kit 2.0 (Pacific Biosciences, Menlo Park, California, USA) according to the manufacturer

127 protocol. The finished library was sequenced at the USDA-ARS Genomics and Bioinformatics
128 Research Unit in Stoneville, Mississippi, USA, where the polymerase binding reaction was
129 performed and sequencing was carried out on one Pacific Biosciences 8M SMRT Cell on a
130 Sequel IIe system (Pacific Biosciences, Menlo Park, California, USA) using a 30-hour movie
131 collection time after a 2-hour pre-extension. Following sequence collection, consensus sequences
132 from the raw PacBio Sequel IIe subreads was called using the SMRTLink v8.0 software (Pacific
133 Biosciences, Menlo Park, California, USA).

134 To complement the PacBio HiFi sequencing, enriched chromosome conformation capture
135 (HiC) sequencing was performed using another *D. similis* eonymph male sample from the same
136 clutch of progeny from a single unmated *D. similis* female (*D. similis* is arrhenotokous, and
137 virgin females produce haploid, male-only families). The Arima HiC kit (Arima Genomics, San
138 Diego, California, USA) was used to perform the proximity ligation after initial crosslinking
139 using the Arima HiC low input protocol. Proximity-ligated DNA was sheared using a Bioruptor
140 (Diagenode, Denville, New Jersey, USA), and appropriately sized fragments (200-600 bp) were
141 selected as the input for the Illumina library preparation using the Swift Accel NGS 2S Plus kit
142 (Integrated DNA Technologies, Coralville, Iowa, USA). The final library was sequenced on a
143 fraction of a lane of NovaSeq 6000 with 150 bp paired-end sequencing. Adapter trimming was
144 performed using BaseSpace software (Illumina, San Diego, California, USA).

145

146 *Genome assembly*

147 Adapter-contaminated HiFi reads were filtered from the circular consensus sequencing
148 (CCS) dataset using HiFiAdapterFilt v2.0 (Sim et al, 2022). Filtered CCS reads were assembled
149 into a contig assembly using HiFiASM v0.16.1-r375 (Cheng et al. 2021) with no modifications

150 to the default parameters. The default output of HiFiASM is a contig assembly displayed in
151 graphical fragment assembly (gfa) format which was converted to fasta format using any2fasta
152 (Seeman, 2018). Due to the extremely high contiguity of the contig assembly, the assembly was
153 manually scaffolded using HiC data, employing the Phase Genomics HiC functions (Kronenberg
154 and Sullivan, 2018, phasegenomics.github.io,
155 https://github.com/phasegenomics/juicebox_scripts) (Phase Genomics, Seattle, Washington,
156 USA) and Juicebox assembly tools (Dudchenko et al. 2017). The HiC reads were mapped to the
157 contig assembly using bwa mem and purged of PCR duplicate artifacts using samblaster. The
158 resulting bam file was converted into a hic formatted file using a combination of Matlock, which
159 generates a links file, which is then converted to a .hic file using `run-assembly-visualizer.sh`
160 from 3d-dna. The HiC data was then used to manually join and edit contigs into chromosomes
161 using Juicebox v1.11.08 (Durand et al. 2015) and the edits were applied to the contig assembly
162 using juicebox_assembly_converter.py by Phase Genomics.

163

164 *Assembly quality analysis*

165 Assembly quality was assessed using metrics for completeness in terms of gene content,
166 artifact duplicate content, parity with estimated genome size, and taxonomic assignment of each
167 assembled fragment. Completeness and amount of duplication were assessed by identifying
168 presence of a benchmark of universal single-copy ortholog (BUSCO) genes from the Eukaryota,
169 Metazoa, Arthropoda, Insecta, Endopterygota, and Hymenoptera odb10 databases through *ab*
170 *initio* gene prediction of the assembly using Metaeuk v.4.a0f584d (Levy et al. 2020) for all the
171 ortholog databases except for the Metazoa database which required annotation using Augustus
172 v3.4.0 (Stanke et al. 2008). Annotations and designations of whether the orthologous genes were

173 found in complete single copy, duplicated, fragmented, or missing were evaluated using BUSCO
174 v5.2.2 (Manni et al. 2021) in `genome` mode. Genome size was estimated using k-mer
175 abundance calculated using KMC v3.2.1 (Kokot et al. 2017) and analyzed using GenomeScope
176 v.2.0 (Ranallo-Benavidez, 2020). Genome coverage was estimated using KAT v2.4.2 (Mapleson
177 et al. 2017) which uses k-mer abundance and spectra analysis to assess ploidy, coverage depth,
178 and amount of duplication in the assembly relative to the raw reads. Finally, taxonomic
179 assignment of each assembly scaffold or contig was determined by local alignment using
180 nucleotide-nucleotide BLAST v2.5.9+, `blastn` (Camacho et al. 2009) to the NCBI nt database
181 (accessed on 2017-06-05) and Diamond v.2.0.9.147, `diamond blastx` (Buchfink et al. 2021) to
182 the UniProt Reference Proteomes database (accessed on 2020-03). Local alignment results were
183 used to assign scaffolds and contigs to taxa using the blobtools v.2.6.1(Challis, et al. 2020)
184 taxrule function `bestsumorder` which assigns taxonomic identity first based on nucleotide
185 BLAST hit followed by the proteome BLAST hit. Scaffold and contig coverage was determined
186 by mapping the raw reads back to the assembly using minimap2 v2.2-r1101 (Li, 2021). Results
187 from the BUSCO analyses, alignments to the nucleotide and proteome databases, and read
188 coverage were summarized using blobblurb (Sim, 2022).

189

190 *WGS Sample collection, DNA extraction, library prep, and sequencing*

191 We extracted and sequenced DNA from 84 *Diprion similis* individuals collected across
192 77 sites on six different pine hosts (Table S1). Our sampling scheme was chosen to maximize the
193 geographic and host range of available preserved samples, consistent with our overall goal of
194 evaluating broad-scale demographic patterns across the introduced range. All samples were
195 obtained from preserved larvae or adult females collected between 2001 and 2020 and stored in

196 95-100% ethanol at -20 °C until use. Individuals were dissected to avoid contamination from the
197 midgut (in the case of larvae) or eggs (in the case of adult females) and then DNA was extracted
198 using Qiagen DNeasy Tissue Kits (Qiagen Inc., Valencia, CA, USA). DNA concentrations were
199 then assessed using a Qubit 2.0 fluorometer (Invitrogen, Waltham, MA, USA).

200 Library preparation and next-generation sequencing were performed on all 84 samples at
201 Admera Health (South Plainfield, NJ, USA). Library prep was performed using KAPA
202 HyperPrep (Roche, Basel, Switzerland) kits. Each sample was sequenced using 150 bp paired-
203 end reads on an Illumina Novaseq 6000 S4 flowcell (Illumina, San Diego, CA).

204

205 *Data filtering: hard-genotype calls, contamination, and haploid males*

206 Raw, demultiplexed reads were first processed using Trimmomatic (v0.3; Bolger et al.
207 2014) to trim adapter sequences from the ends of reads. Reads were then aligned to the *Diprion*
208 *similis* reference genome using the end-to-end alignment option of Bowtie2 (v2.2.3, Langmead
209 and Salzberg 2012). We then used Samtools (v0.1.19; Li et al. 2009) to exclude reads that
210 mapped to more than one location in our reference genome.

211 Because downstream analyses assume diploidy for all samples and diprionid sawflies—
212 like all hymenopterans—have haplodiploid sex determination, we removed putative haploid
213 males from our dataset. However, most of our samples were preserved larvae, which we cannot
214 sex reliably, and pine-sawfly males can occasionally be diploid (Harper et al. 2016; Bagley et al.
215 2017). We therefore used heterozygosity to infer ploidy. To do so, we obtained hard-genotype
216 calls using mpileup from bcftools (v1.19, Li et al. 2011) and the -het option in vcftools (v1.19
217 Danacek et al. 2011). While processing these data, we found evidence of small amounts of
218 contamination in samples—indicated by skewed allele counts unlikely to be the result of true

219 heterozygosity. To address this, sites with skewed allele counts were flagged in each individual
220 as missing data for downstream filtering. We then removed any site where more than half the
221 individuals had missing data, retaining only sites with 5x individual depth of coverage and a
222 minimum base Phred score of 20. After filtering for contamination, we examined patterns of
223 heterozygosity across individuals, we excluded 20 individuals with <0.02 heterozygosity as
224 putative haploid males, for a final dataset of 64 diploid individuals (Table S2).

225

226 *ANGSD genotype-likelihood estimation*

227 To account for genotype uncertainty in downstream analyses—a recommended strategy
228 for analyzing WGS datasets with coverage as low as 1x (Lou et al. 2020)—we used ANGSD
229 (v0.933, Korneliussen et al. 2014). This program produces genotype-likelihood estimates in lieu
230 of “hard” single-nucleotide polymorphism (SNP) calls, and these genotype likelihoods were used
231 for most downstream analyses (but see below). For our dataset, genotype likelihoods were
232 estimated after keeping sites where >50% of samples passed filters for minimum mapping
233 quality and base quality of 20, minor allele frequency > 0.05, minimum coverage depth of 1x,
234 and maximum coverage depth of 100x (to remove repetitive loci). We then pruned using linkage
235 disequilibrium calculated from genotype likelihoods using ngsLD (v1.1.1, Fox et al. 2019),
236 which estimates linkage disequilibrium across the genome to produce a list of unlinked SNPs.
237 With this list, we used ANGSD to estimate genotype likelihoods only for unlinked SNPs for use
238 in downstream analyses. However, two analyses—isolation by distance and heterozygosity (see
239 below)—required “hard” SNP calls instead of likelihoods. To facilitate this, ANGSD was re-run
240 with the -dobcf and -dogeno options to produce a bcf file with “hard” SNPs at the same sites as

241 the genotype-likelihood approach. This approach kept all the same sites as used in the genotype-
242 likelihood approach, as these sites were already filtered.

243

244 *Evaluation of discrete population structure: PCA and NgsAdmix*

245 Population structure within the introduced range of *D. similis* was inferred by two
246 individual-based approaches that use genotype likelihoods and are implemented as extensions of
247 the ANGSD platform. First, we used the program PCAngsd (v1.03, Meisner and Albrechtsen
248 2018) to estimate the genetic covariance matrix and perform a principal component analysis
249 (PCA) on low-coverage genotype-likelihood data. This approach allows visualization and
250 analysis of genetic clustering via admixture estimation from principal axes of genetic variation.
251 Based on patterns revealed in this and other structure analyses (see below and *Results*), we also
252 used the *lm* function of base R (version 4.2.0 R Core Team 2022) to model the first principal
253 component eigenvector (PC1) as a function of geography (longitude of sample location). To infer
254 the number of populations (K) based on the PCA analysis, we chose the value of K that was one
255 fewer than the number of eigenvalues that pass Velicer's minimum average partial (MAP) test,
256 following (Shriner 2011). To explore an alternative clustering solution, we also used the -admix
257 command and the first 10 eigenvectors of the PCA to estimate admixture proportions for each
258 individual for $K=2$.

259 For our second approach to evaluating discrete population structure, we used NgsAdmix
260 (v33), which calculates individual admixture proportions from low-coverage NGS data by
261 accounting for uncertainty present in genotype likelihoods (Skotte et al. 2013). Because we have
262 no *a priori* prediction for K , we ran NgsAdmix with a range of K values from 1 to 7, with 10
263 independent runs for each value of K . We then computed the average resulting likelihoods for

264 each K value to evaluate the most likely optimal K value. As was done for the PCA-based
265 approach, we also examined admixture proportions for the second-best clustering solution, $K=2$.

266

267 *Evidence of continuous population structure (isolation-by-distance)*

268 To determine whether there is evidence of isolation-by-distance (IBD) in the introduced
269 range, we first generated geographic and genetic matrices using SPAGEDI (v1.5b; Hardy &
270 Vekemans 2002). Because our individuals were not sampled from discrete populations, we
271 calculated pairwise genetic distances Rousset's \hat{a} which is analogous to the $F_{ST}/(1 - F_{ST})$ ratio
272 (Rousset 2000). Briefly, for a pair of individuals i and j , Rousset's distance \hat{a} is given by $a_{ij} =$
273 $(Q_w - Q_{ij})/(1 - Q_w)$, where Q_{ij} is the probability of identity by state of gene copies between
274 individuals and Q_w is the probability of identity within individuals (estimated from all pairs of
275 individuals in the sample). We calculated pairwise Rousset's \hat{a} (Rousset 2000) using a set of
276 10,000 loci randomly downsampled from our “hard” SNP call data (see above) to comply with
277 the maximum number of loci allowed by SPAGEDI 1.5. This program also calculated a pairwise
278 linear geographic distance matrix between latitude and longitude coordinates of individuals. To
279 test for IBD, we used the genetic and geographic distance matrices and the `mantel.randtest()`
280 function from the `ade4` package of R (v1.7, Dray and Dufour 2007) to perform a Mantel test
281 (Mantel 1967) with 10,000 permutations.

282

283 *Spatial patterns of heterozygosity*

284 To investigate how genetic diversity changes as a function of distance from the
285 hypothesized location of introduction, we used individual heterozygosity estimates using the
286 `vcftools -het` option on the “hard” genotype dataset (see above) as our measure of genetic

287 diversity. For spatial distance from the origin of the invasive population, we used New Haven,
288 Connecticut, United States (latitude: -73, longitude: 41.28) as the introduction site, in accordance
289 with museum records of the species invasion (Britton 1915). We then calculated distance in
290 kilometers from New Haven to each collection site using the geodist package in R (v0.0.7,
291 Padgham et al. 2021). To evaluate the relationship between heterozygosity and distance from
292 CT, we used the *lm* function of R to fit a linear model to the data.

293

294 **Results**

295 *Diprion similis de novo genome assembly*

296 The *D. similis* iyDipSim1.1 (NCBI project: [JAJNQI01](#)) haploid assembly was sequenced
297 to 100x coverage, producing an assembly size of 270.225 MB in 14 haploid chromosomes
298 (consistent with published karyotype descriptions, Rousselet et al. 1998), 81 scaffolds, and 93
299 total contigs (see Table S3). The final genome size was slightly larger than the GenomeScope
300 estimate based on k-mer abundance (Figure S1), though the larger than expected assembly was
301 unlikely due to the inclusion of duplicate fragments (Figure S2), but rather short unplaced
302 heterochromatic regions with an elevated GC content (Figure S3). In the final chromosome-
303 length assembly, the smallest scaffold necessary to make up 50% of the genome (N50) was
304 19.014 MB, and size of the smallest scaffold necessary to make up 90% of the genome (N90)
305 was 11.122MB (Figure S4). Completeness in terms of BUSCO annotation ranged from 91.5% of
306 the Hymenoptera v.10 orthologs to 95.6% of the Arthropod v.10 orthologs. Of the Hymenoptera
307 BUSCOs, all complete genes found in single copy (n = 5457 genes) or duplicated (n = 25) were
308 in assembled chromosomes with none found in unplaced contigs. Analysis of local alignments to

309 the NCBI nucleotide and UniProt Proteomes databases revealed no fragments from non-*D.*
310 *similis* species in the assembly (Figure S3, Table S4).

311

312 *WGS sequencing, haploid filtering, and genotype-likelihood estimation.*

313 After sequencing, we obtained an average of 24.09 +/- 13.3 (SD) million reads per
314 individual. An average of 22.59 +/- 12.84 of these reads mapped to the reference genome after
315 removing duplicates and paralogs, and these reads covered an average of 94.3% of the reference
316 genome. Following filtering for contamination, site depth, and base quality, we identified 22
317 putative haploid samples with markedly low (<0.02, Figure S5) heterozygosity that were
318 removed from downstream analyses (Table S2). For the remaining 64 samples we filtered sites
319 for mapping and base quality, minor allele frequency, minimum coverage of 1x, and maximum
320 coverage of 100x, resulting in genotype likelihoods for 728,627 variable sites. After pruning
321 based on linkage disequilibrium, we retained 352,385 genotype likelihoods for unlinked SNPs
322 for downstream analysis. An analogous dataset with “hard” genotyped SNPs at the same sites
323 was also used for IBD and heterozygosity analyses.

324

325 *Discrete population structure, isolation-by-distance, and heterozygosity*

326 Analyses using PCAangsd and NgsAdmix both selected $K=1$ as the optimal number of
327 genetic clusters in this dataset. For the PCA-based approach, $K=1$ was supported by the
328 observation that only two eigenvectors passed the MAP test (Shriner 2011). Visualization of
329 these two eigenvectors (principal components) indicates that much of the variation is explained
330 by PC1 (10.5% of overall variance, Figure 2A), which correlates strongly with geography (linear
331 model: $F = 69.2$, $P < 0.001$, $R^2 = 0.527$, Figure 2B). PC2 appears to explain additional variation

332 among individuals sampled from the eastern portion of the range, closer to the presumed
333 invasion site, but no strong geographic patterns emerge from further dissecting this axis (Figure
334 1C). For the NgsAdmix analysis, $K=1$ was supported by likelihood values from 10 replicate runs,
335 which matched our results from PCAngsd (Figure S6).

336 To further evaluate the potential for substructure in the data, we also evaluated population
337 assignments (admixture proportions) for the next best clustering solution, $K=2$. Both PCAngsd
338 and NgsAdmix produced very similar admixture proportions, with a continuous transition in
339 admixture proportions between eastern and western groups (Figure S7). The lack of a discrete
340 break between the two groups for the $K=2$ clustering solution (Figure S7) is consistent with a
341 pattern of isolation-by-distance in a single continuous population (Miermans 2012).

342 To evaluate evidence for isolation-by-distance in the introduced range, we used Mantel
343 tests, which revealed that there was significant positive relationship between genetic distance and
344 geographic distance ($R^2 = 0.562$, $P < 0.0001$, Figure 3). Plotting pairwise genetic and geographic
345 distances also revealed some discontinuities in the IBD relationship, with two somewhat distinct
346 clusters of points (Figure 3A). The smaller cluster of points near 0 genetic distance and < 500 km
347 from each other represents the enriched sampling in the north-west edge of *D. similis*' range. The
348 discontinuity seen between this and the larger cloud of points in the IBD figure might therefore
349 be explained by gaps in sampling; increasing sampling east and south of these locations could
350 bridge this gap.

351 Finally, across the 64 diploid females, average observed heterozygosity was 0.186
352 (Figure S5). We found that heterozygosity was significantly correlated with geographic distance
353 from the presumed location of first introduction in New Haven, CT, USA ($F = -2.47$, $P = 0.0162$,
354 $R^2 = 0.075$), with individuals further from this point showing reduced diversity (Figure 3B).

355

356 **Discussion**

357 Analyses of population structure in successful biological invasions are essential for
358 understanding the demographic and evolutionary processes behind these “natural experiments”
359 (Lee 2002, Sakai et al. 2001, Yoshida et al. 2007). But accurate analysis of population structure
360 may require genomic datasets consisting of many unlinked markers (Sherpa et al. 2018, Lewald et
361 al. 2021). Moreover, if detection of locations in the genome that have undergone recent positive
362 selection is a goal, whole-genome data are better suited to the task than reduced-representation
363 data (reviewed North et al. 2021). As a first step to developing *Diprion similis* as a model system
364 for invasion biology, we assembled a high-quality reference genome and generated low-coverage
365 WGS data for 64 diploid (female) individuals sampled across the introduced range of *D. similis*
366 in North America. We found strong evidence for a single North American population of this
367 species, with a pattern of isolation-by-distance in the introduced range. Here, we discuss both the
368 limitations and implications of our data, while also highlighting future directions that leverage *D.*
369 *similis* as a model for investigating genomics of adaptation following biological introduction.

370

371 *Spatial patterns of genetic variation support a single-invasion scenario*

372 Our main purpose for describing population structure in North American *D. similis* was
373 to distinguish between single-invasion and multiple-invasion scenarios, an essential first step to
374 understanding how invasive populations adapted to a novel pine, *Pinus strobus*. We evaluated
375 three predictions for a single-invasion scenario. First, a single wave of invasion should yield
376 population structure with a single genetic cluster in the introduced range, while subsequent
377 invasions are readily identified as separate genetic groups (van Boheeman et al. 2017). Our

378 analyses identified $K=1$ —a single genetic cluster—as the mostly likely number of populations
379 within the introduced range of *D. similis*. Further supporting a single-invasion scenario,
380 population assignments for the next-best clustering solution ($K=2$) produced a continuous
381 gradient of population membership rather than a discrete break between two isolated populations
382 (Figure 2A). Second, genetic relationships between individuals in the introduced range are
383 expected to follow a continuous isolation-by-distance (IBD) pattern only if a single invasion
384 occurred (Sherpa et al. 2018). This predicted pattern of IBD is evident in North American *D.*
385 *similis* (Figure 3A), with most admixture and gene flow occurring between spatially contiguous
386 areas throughout the range. This indicates that in the hundred years following a single
387 introduction, the introduced meta-population is at or near drift-migration equilibrium (Sherpa et
388 al. 2018). Third, in a single introduction scenario, genetic diversity is expected to decrease as the
389 invasion spreads away from the original point of introduction, due to small population sizes and
390 genetic drift at the edges of range expansions (Van Petegem et. al 2017, Biolozyt et al. 2005,
391 Hewitt 1993). Consistent with this, there is a subtle—but significant—decline in heterozygosity
392 with distance from the assumed point of introduction in New Haven, CT (Figure 3B).

393 While our data strongly support a single introduction scenario, several limitations of our
394 dataset should be considered. One limitation of our population structure analyses is that we have
395 not yet sampled populations in the ancestral range, making it impossible to evaluate potential
396 source populations for the North American *D. similis* invasion. Another limitation is that there
397 are several small, but potentially meaningful sampling gaps across the introduced range of *D.*
398 *similis* (Figure 1C). Thus, we cannot rule out the possibility that there are genetically distinct
399 populations that we did not sample. However, apart from not having samples from very recent
400 appearances in the northwestern USA (Looney et al. 2016), our samples span most of the North

401 American range of *D. similis*, and our largest sampling gaps were primarily located in the middle
402 of this range. This type of sampling gap—which would be expected to cause artificial
403 discontinuities in allele frequencies—should bias our results to detecting more populations, not
404 fewer (Meirmans 2012). Moreover, any unsampled populations should still be detectable via
405 admixture with nearby populations and via disruption of IBD and heterozygosity patterns, which
406 we do not observe apart from a minor discontinuity in our IBD plot (Figure 3A). Thus, even with
407 some sampling gaps, our data strongly support the historical description of this invasion (Zappe
408 1917, Middleton 1923, Codella et al. 1991): *D. similis* was first introduced somewhere near New
409 Haven, CT approximately 110 years ago, after which it rapidly spread over a substantial portion
410 of eastern North America.

411

412 *Why are single-introduction scenarios rare?*

413 Our main conclusion that the highly successful *D. similis* invasion likely stems from a
414 single introduction event contrasts with a large body of literature demonstrating that multiple-
415 invasion scenarios are common, and in some cases necessary for successful colonization (Blair et
416 al. 2012, Rius et al 2012, Rosenthal et al. 2008, Kolbe et al. 2007, reviewed Rius and Darling
417 2014). However, most studies evaluating population genomics of invasive species are in systems
418 with much more recent introduction events (<50 years) than the ones investigated here (>100
419 years), and there is some evidence that age of the invasive population may influence patterns of
420 population structure. For example, with a history of multiple invasions of different ages in
421 different areas, the Asian tiger mosquito *Aedes albopictus* offers insights on the relationship
422 between invasion age and population structure. Although *A. albopictus* colonized Pacific and
423 Indian Ocean islands more than a century ago, it was not recorded in Europe until much more

424 recently—Albania in 1979 and Italy in 1990—where it has since expanded across the continent
425 (Scholte and Schaffner 2007, Benedict et al. 2007). Recent work demonstrates that populations
426 from an older invasion on Reunion Island have a continuous IBD pattern, indicative of a single
427 introduction (Sherpa et al. 2019). In contrast, more recently established European populations
428 have a discontinuous pattern of population structure, indicative of multiple, more recent
429 introductions (Sherpa et al. 2018, Sherpa et al. 2019, Schmidt et al. 2020). One possible
430 explanation for differences in population structure between old vs. young invasions is that
431 increased trade globalization makes multiple-invasion scenarios more likely in recent years than
432 they were in the past (Seebens et al. 2015, Sardain et al. 2019).

433 A non-mutually exclusive hypothesis for explaining different patterns of population
434 structure in old vs. young invasions is that evidence of multiple introductions may get erased
435 over time. For example, an older invasive population could have had multiple introductions, but
436 with whole-sale extinction of early invasive populations and replacement by subsequent, more
437 successful introductions. From a genetic variation perspective, however, extinction and
438 replacement via a new introduction with limited admixture is essentially equivalent to a single-
439 invasion scenario. Alternatively, if there has been enough time and sufficient gene flow between
440 invading populations, secondary invasions may not be detectable from samples of modern
441 invasive populations, although samples from source populations—if available—may provide
442 some evidence of historical admixture. Overall, multiple-invasion scenarios may be much harder
443 to detect in older invasions (e.g., >100 years) due to the possibility that introduced populations or
444 source populations have since gone extinct. Fortunately, recent advances in museum genomics
445 (Parejo et al. 2020, reviewed Raxworthy and Smith 2021) may make it possible to resurrect these
446 lost populations. With good representation in natural history literature and museum collections—

447 and now a reference genome for mapping sequencing reads from degraded samples—*Diprion*
448 *similis* provides an excellent test case for using museum genomics to evaluate cryptic multiple-
449 invasion scenarios.

450

451 *Adaptation in single-invasion scenarios*

452 If *Diprion similis* arrived in a single introduction event as the data here suggest, it
453 remains unclear how this species had sufficient genetic variation to shift to white pine (*Pinus*
454 *strobus*) in North America. According to the genetic paradox of invasions, a single invasive
455 wave is expected to considerably reduce genetic diversity (Allendorf and Lundquist 2003,
456 Frankham 2005), thereby limiting the raw genetic material available for adapting to novel hosts.
457 Nevertheless, there are several potential mitigating factors that may explain how invasive
458 populations can adapt to novel environments despite limited genetic variation (Estoup et al.
459 2016). Here, we consider several non-mutually exclusive explanations that may apply to *D.*
460 *similis*. The most plausible of these may be that the introduced range provides no adaptive
461 challenge to the invading species. While *Neodiprion* pine sawfly species that do not ordinarily
462 oviposit on white pine experience increased egg (Bendall et al. 2017) and larval (CRL, personal
463 observation) mortality, the same may not be the case for *D. similis*. For example, unlike
464 *Neodiprion* females, *D. similis* females use resin and pulp from the pine to cover the exposed egg
465 (Zappe 1917, Bittner et al. 2019, Bendall et al. 2017). It is therefore possible that this difference
466 in oviposition behavior is a pre-adaptation for white pine use in *D. similis*. One way to test this
467 hypothesis would be to measure egg-laying success in European populations of *D. similis* that
468 have never been exposed to *P. strobus*.

469 Another mechanism that could account for a rapid host shift despite presumably limited
470 genetic variation is if novel environments in the invasive range releases phenotypic plasticity for
471 host use (Lande 2015, Funk 2008, Zenni et al. 2014). For example, *Pinus sylvestris* is considered
472 the primary host of *D. similis* in its native range, but it has been documented attacking a variety
473 of other pines throughout its range (Codella et al. 1991). Across this range, *P. sylvestris* is the
474 dominant and often sole pine species available for attack, however some locations—particularly
475 in mountainous regions of Europe—having much greater pine diversity (Jin et al. 2021). It is
476 therefore possible that *D. similis* populations subject to environments with greater diversity in
477 pine hosts have increased plasticity in host-use phenotypes. Therefore, if the North American
478 population came from a *D. similis* population with more generalized pine use, pre-existing
479 plasticity for host acceptance—possibly coupled with pre-adaptations for laying eggs in different
480 types of needles—may have facilitated rapid shifts to novel hosts. Testing this hypothesis will
481 require evaluating host preference and acceptance behaviors in potential source populations
482 within the native range of *D. similis*. Other genetic phenomena in founder populations—such as
483 epigenetics and purging of deleterious mutations (Estoup et al. 2016)—can also promote
484 persistence and adaptation in the invasive range. Ultimately, pairing the genomic resources
485 generated here with additional experimental work in native and invasive *D. similis* populations
486 would provide useful insights into the genetic mechanisms underlying host shifts in invasive
487 populations.

488

489 **Conclusion**

490 Overall, our results and discussion highlight the value of taking an integrative approach
491 to evaluating the history of invasions: while genomic data are valuable, their interpretation

492 hinges on their ecological and historical context. Here, we lay the groundwork for establishing
493 *Diprion similis* as a model for evaluating the demographic history and genetic underpinnings of
494 adaptation in biological invasions. Armed with the genomic resources and spatial patterns of
495 genetic variation presented here, future work can leverage two key advantages in this system: (1)
496 a rich collection of historical samples and data that will provide snapshots of genetic variation in
497 past *D. similis* populations, and (2) experimental tractability for connecting genetic variation to
498 ecologically relevant traits and their impact on fitness. Ultimately, this work will answer pressing
499 questions about prevalence of single invasion scenarios and consequences for adaptation to novel
500 environments.

501

502 **Data Availability**

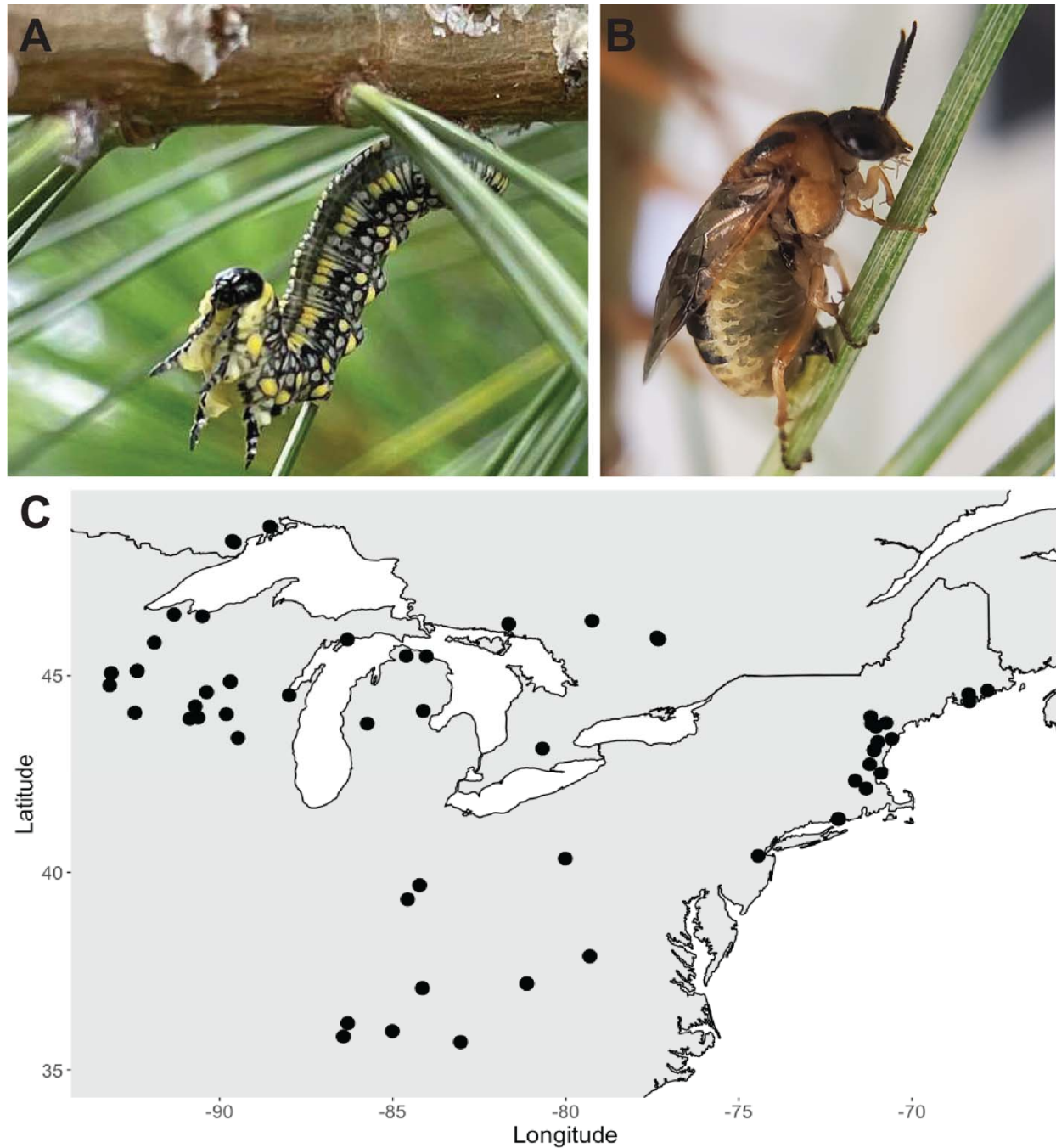
503 The *de novo* assembled reference genome can be found on NCBI (BioProject
504 [PRJNA784632](#)). Additional data, including individual WGS sequences for all 64 samples,
505 genotype-likelihood .beagle file, and hard-called genotype data in .vcf format can be found on
506 Dryad repository upon publication.

507 **Funding**

508 This work was supported by the National Science Foundation: Postdoctoral Research
509 Fellowship in Biology-2010660 (JSD and CRL), DEB-1257739 (CRL), and DEB-CAREER-
510 1750946 (CRL); USDA Agricultural Research Service project number 2040-22430-028-00-D
511 and SCINet project number 0500-00093-001-00-D; and an American Genetics Association
512 Evolutionary, Ecological, or Conservation Genomics Research Award (JSD).

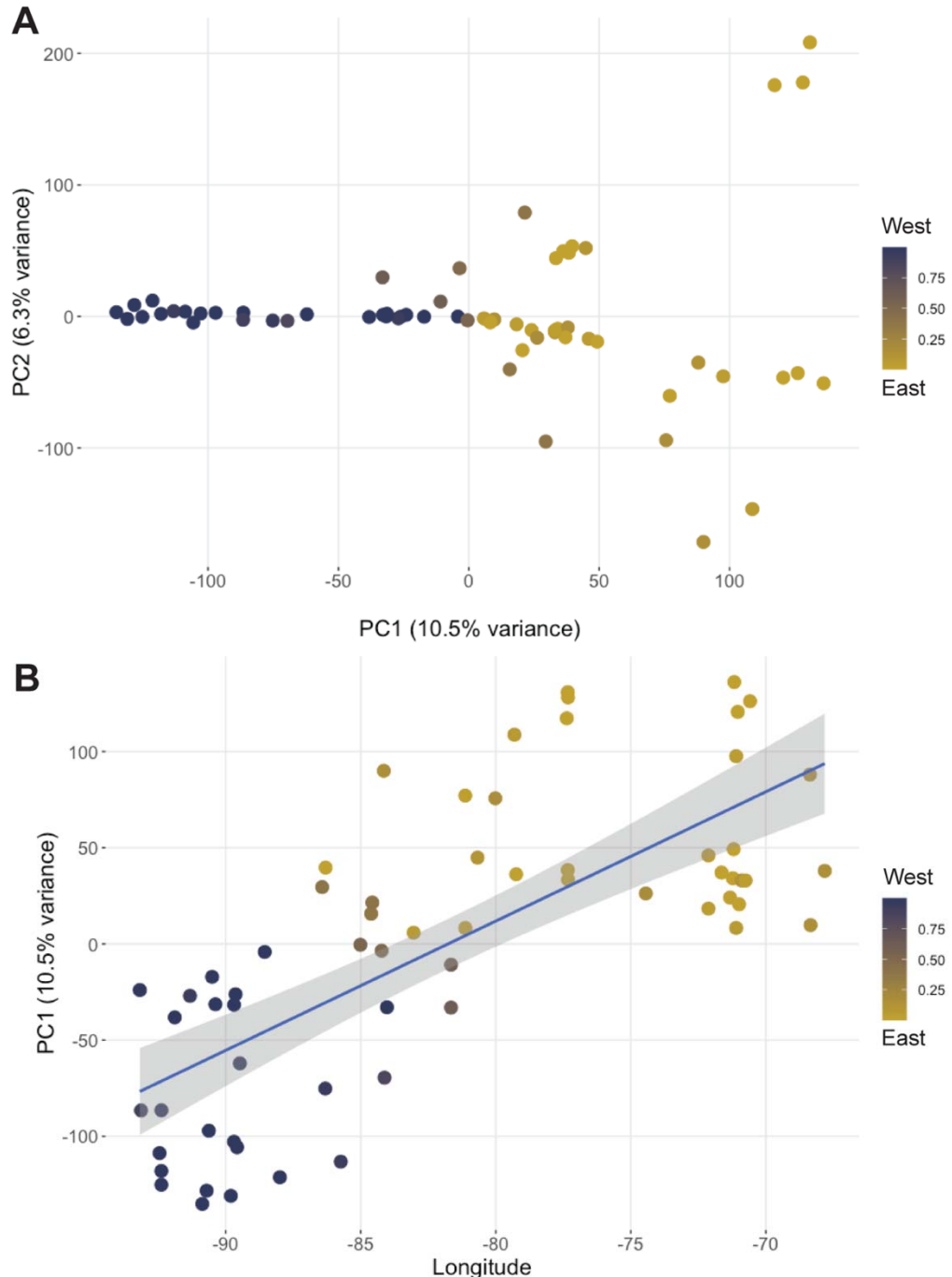
513 **Acknowledgements**

514 We thank current and former Linnen lab members: Robin Bagley, John Terbot, and
515 Ashleigh Glover for collecting and providing many of the samples used in this work. We thank
516 Jane Dostart for permission to use her photograph of a *Diprion similis* larva as well as excellent
517 care of insects. We thank Dr. David Smith of the Smithsonian National Museum of Natural
518 History for helpful comments on availability and richness of museum collections for this species.
519 The authors thank the members of the USDA-ARS Ag100Pest Team for sequencing and analysis
520 support. All opinions expressed in this paper are the author's and do not necessarily reflect the
521 policies and views of USDA. Mention of trade names or commercial products in this publication
522 is solely for the purpose of providing specific information and does not imply recommendation
523 or endorsement by the U.S. Department of Agriculture.



524
525
526
527
528

Figure 1: A) Photo of late-instar *Diprion similis* larva on white pine. Photo by Jane Dostart. B) Photo of *D. similis* adult female ovipositing eggs on white pine (*Pinus strobus*). C) Sampling locations of *Diprion similis* in eastern North America (United States and Canada) used for WGS.

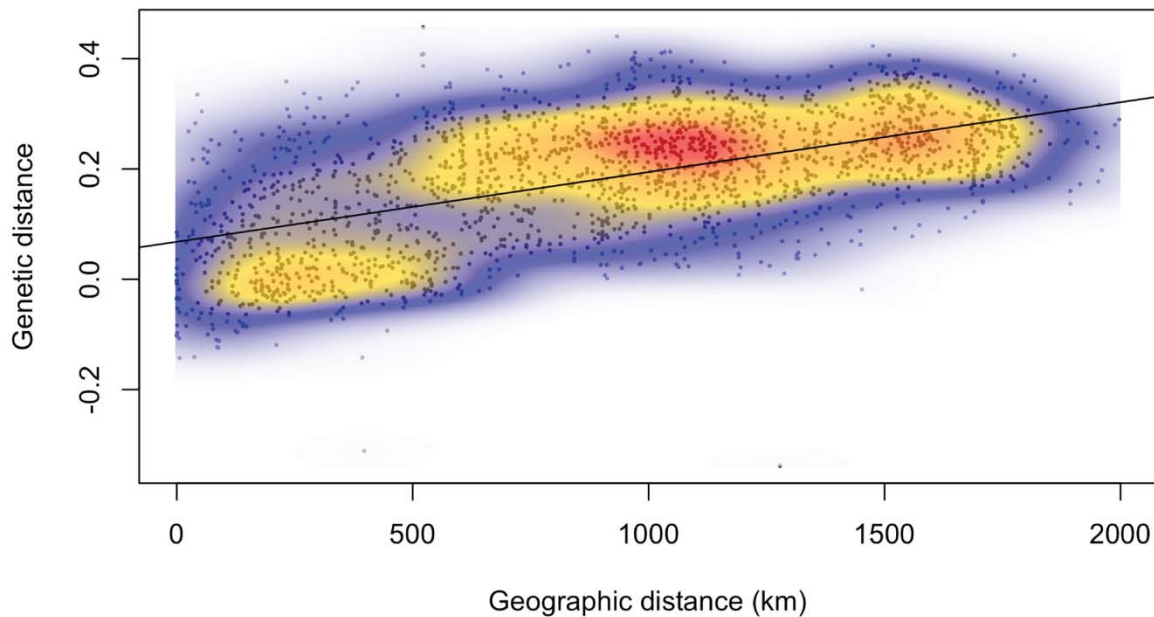


529
530
531
532
533
534
535
536
537
538

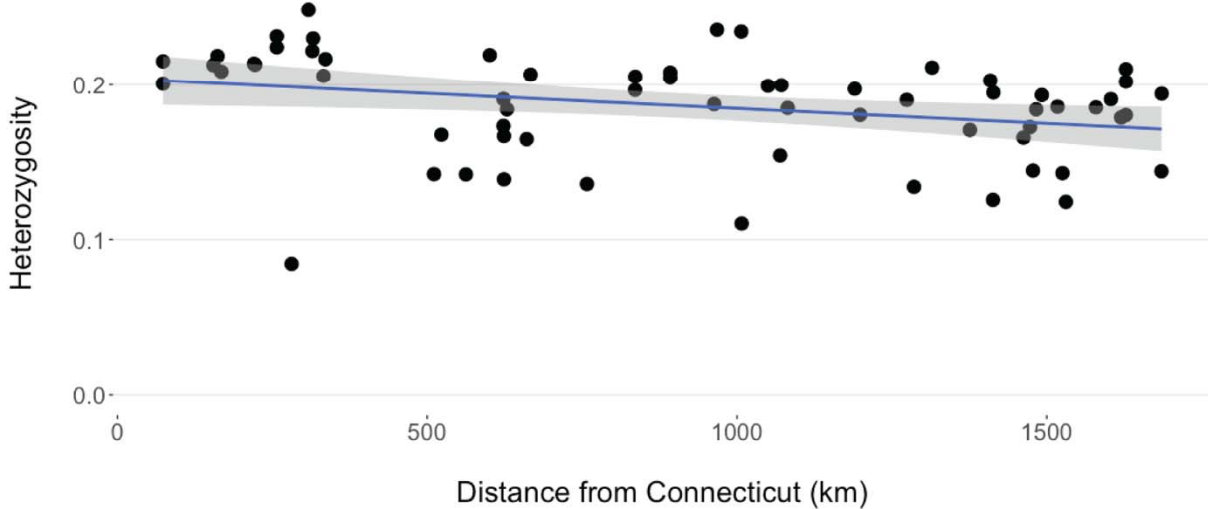
Figure 2: Results of PCAgnsd analysis of population structure. A) Principal component axes of genetic variation from samples, as calculated by PCAgnsd. The color shading of individual points in both panels shows admixture proportion as determined by PCAgnsd for K=2 and analogous to the admixture proportions shown in Figure S7. Note that K=1 is the optimal clustering solution, admixture proportions for K=2 are shown to highlight the lack of a discrete break corresponding to two clusters. Panel A shows the component axes with highest contribution of overall variance, with PC1 inverted to align better with geographic orientation. **B)** PC1 as a function of longitude of origin for each sample, and these variables are significantly correlated (linear model: $F = 69.2$, $P < 0.001$, $R^2 = 0.5274$).

A

Isolation by distance across North America



B



539
540
541
542
543
544
545
546
547
548

Figure 3: Spatial patterns of genetic variation in North American *D. similis*. **A)** Heatmap for isolation by distance (IBD) between all samples in the introduced range. Axes measure pairwise geographic and genetic distances in km and Rousset's $\hat{\alpha}$ respectively. Localized density between more-related individuals is indicated by warmer colors on the plot. Mantel tests indicate significant IBD range-wide ($R^2 = 0.562, P < 0.0001$). These results indicate continuous isolation by distance. **B)** Spatial pattern to genetic diversity from the assumed original point of introduction in New Haven, CT. The Y-axis uses heterozygosity as a measure of genetic diversity for each individual sample. The correlation between these variables is significant (linear model: $F = -2.47, P = 0.0162, R^2 = 0.075$).

549 **References**

550

551 Allendorf, F. W., & Lundquist, L. L. (2003). Introduction: Population biology, evolution, and
552 control of Invasive Species. *Conservation Biology*, 17(1), 24–30.
553 <https://doi.org/10.1046/j.1523-1739.2003.02365.x>

554 Bagley, R. K., Sousa, V. C., Niemiller, M. L., & Linnen, C. R. (2017). History, geography and
555 host use shape genomewide patterns of genetic variation in the redheaded pine sawfly
556 (*Neodiprion lecontei*). *Molecular Ecology*, 26(4), 1022–1044.
557 <https://doi.org/10.1111/mec.13972>

558 Bendall, E. E., Bagley, R. K., Sousa, V. C., & Linnen, C. R. (2022). Faster-haplodiploid
559 evolution under divergence-with-gene-flow: Simulations and empirical data from pine-
560 feeding hymenopterans. *Molecular Ecology*, 31(8), 2348–2366.
561 <https://doi.org/10.1111/mec.16410>

562 Bendall, E. E., Vertacnik, K. L., & Linnen, C. R. (2017). Oviposition traits generate extrinsic
563 postzygotic isolation between two pine sawfly species. *BMC Evolutionary Biology*,
564 17(1), 1–15. <https://doi.org/10.1186/s12862-017-0872-8>

565 Benedict, M., Levine, R., Hawley, W., & Lounibos, L. (2007). Spread of the tiger: Global risk of
566 invasion by the mosquito *Aedes albopictus*. *Vector-Borne and Zoonotic Diseases*, 7(1),
567 76–85.

568 Bialozyt, R., Ziegenhagen, B., & Petit, R. J. (2006). Contrasting effects of long distance seed
569 dispersal on genetic diversity during range expansion. *Journal of Evolutionary Biology*,
570 19(1), 12–20. <https://doi.org/10.1111/j.1420-9101.2005.00995.x>

571 Bittner, N., Hundacker, J., Achotegui-Castells, A., Anderbrant, O., & Hilker, M. (2019). Defense
572 of Scots pine against sawfly eggs (*Diprion pini*) is primed by exposure to sawfly sex
573 pheromones. *Proceedings of the National Academy of Sciences of the United States of
574 America*, 116(49), 24668–24675. <https://doi.org/10.1073/pnas.1910991116>

575 Blair, A. C., Blumenthal, D., & Hufbauer, R. A. (2012). Hybridization and invasion: An
576 experimental test with diffuse knapweed (*Centaurea diffusa* Lam.). *Evolutionary
577 Applications*, 5(1), 17–28. <https://doi.org/10.1111/j.1752-4571.2011.00203.x>

578 Bock, D. G., Caseys, C., Cousens, R. D., Hahn, M. A., Heredia, S. M., Hübner, S., Turner, K. G.,
579 Whitney, K. D., & Rieseberg, L. H. (2015). What we still don't know about invasion
580 genetics. *Molecular Ecology*, 24(9), 2277–2297. <https://doi.org/10.1111/mec.13032>

581 Britton, W. E. (1916). Further Notes on Diprion Simile Hartig. *Journal of Economic
582 Entomology*, 9(2), 281–282. <https://doi.org/10.1093/jee/9.2.281>

583 Britton, W. E. (1915). A Destructive Pine Sawfly Introduced from Europe. *Journal of Economic
584 Entomology*, 8(3), 379–382. <https://doi.org/10.1093/jee/8.3.379>

585 Britton WE; Zappe MP, 1918. The imported pine sawfly; *Diprion (Lophyrus) simile* Hartig.
586 Conn. Agr. Exp. Sta. Bull. 203:273-290.

587 Buchfink, B., Reuter, K., & Drost, H. G. (2021). Sensitive protein alignments at tree-of-life scale
588 using DIAMOND. *Nature Methods*, 18(4), 366–368. [https://doi.org/10.1038/s41592-021-01101-x](https://doi.org/10.1038/s41592-021-
589 01101-x)

590 Camacho, C., Coulouris, G., Avagyan, V., Ma, N., Papadopoulos, J., Bealer, K., & Madden, T.
591 L. (2009). BLAST+: Architecture and applications. *BMC Bioinformatics*, 10, 1–9.
592 <https://doi.org/10.1186/1471-2105-10-421>

593 Capinha, C., Essl, F., Seebens, H., Moser, D., & Miquel, H. (2022). The dispersal of alien
594 species redefines biogeography in the Anthropocene Published by : American

595 Association for the Advancement of Science Linked references are available on JSTOR
596 for this article : The The dispersal dispersal of of alien alien species . Science, 348(6240),
597 1248–1251.

598 Carlton, J. T., & Geller, J. B. (1993). Ecological Roulette : The Global Transport of
599 Nonindigenous Marine Organisms. Science, 261(5117), 78–82.

600 Challis, R., Richards, E., Rajan, J., Cochrane, G., & Blaxter, M. (2020). BlobToolKit -
601 interactive quality assessment of genome assemblies. G3: Genes, Genomes, Genetics,
602 10(4), 1361–1374. <https://doi.org/10.1534/g3.119.400908>

603 Cheng, H., Concepcion, G. T., Feng, X., Zhang, H., & Li, H. (2021). Haplotype-resolved de
604 novo assembly using phased assembly graphs with hifiasm. Nature Methods, 18(2), 170–
605 175. <https://doi.org/10.1038/s41592-020-01056-5>.Haplotype-resolved

606 Clavero, M., & Garcia-Berthou, E. (2005). Invasive species are a leading cause of animal
607 extinctions. Trends in Ecology and Evolution. TRENDS in Ecology & Evolution, 20(3),
608 110.

609 Codella, S., Fogal, W., & Raffa, K. (1991). The effect of host variability on growth and
610 performance of the introduced pine sawfly, Diprion similis. Canadian Journal of Forest
611 Research, 21, 1668–1674.

612 Codella, S. G., & Raffa, K. F. (2002). Desiccation of Pinus foliage induced by conifer sawfly
613 oviposition: Effect on egg viability. Ecological Entomology, 27(5), 618–621.
614 <https://doi.org/10.1046/j.1365-2311.2002.00447.x>

615 Coppel, H., Mertins, J., & Harris, J. (1974). The introduced pine sawfly, Diprion similis (Hartig)
616 (Hymenoptera: Diprionidae). A review, with emphasis on studies in Wisconsin.
617 University. University of Wisconsin Research Division, R2393.

618 Danecek, P., Auton, A., Abecasis, G., Albers, C. A., Banks, E., DePristo, M. A., Handsaker, R.
619 E., Lunter, G., Marth, G. T., Sherry, S. T., McVean, G., & Durbin, R. (2011). The variant
620 call format and VCFtools. Bioinformatics, 27(15), 2156–2158.
621 <https://doi.org/10.1093/bioinformatics/btr330>

622 Dlugosch, K. M., & Parker, I. M. (2008). Founding events in species invasions: Genetic
623 variation, adaptive evolution, and the role of multiple introductions. Molecular Ecology,
624 17(1), 431–449. <https://doi.org/10.1111/j.1365-294X.2007.03538.x>

625 Dlugosch, K. M., Anderson, S. R., Braasch, J., Cang, F. A., & Gillette, H. D. (2015). The devil is
626 in the details: Genetic variation in introduced populations and its contributions to
627 invasion. Molecular Ecology, 24(9), 2095–2111. <https://doi.org/10.1111/mec.13183>

628 Dray, S., & Dufour, A. B. (2007). The ade4 package: Implementing the duality diagram for
629 ecologists. Journal of Statistical Software, 22(4), 1–20.
630 <https://doi.org/10.18637/jss.v022.i04>

631 Dudchenko, O., Batra, S. S., Omer, A. D., Nyquist, S. K., Hoeger, M., Durand, N. C., Shamim,
632 M. S., Machol, I., Lander, E. S., Aiden, A. P., & Aiden, E. L. (2017). De novo assembly
633 of the Aedes aegypti genome using Hi-C yields chromosome-length scaffolds. Science,
634 356(6333), 92–95. <https://doi.org/10.1126/science.aal3327>.De

635 Durand, N. C., Shamim, M. S., Machol, I., Rao, S. S. P., Huntley, M. H., Lander, E. S., & Aiden,
636 E. L. (2016). Juicer Provides a One-Click System for Analyzing Loop-Resolution Hi-C
637 Experiments. Cell Systems, 3(1), 95–98. <https://doi.org/10.1016/j.cels.2016.07.002>

638 Ekblom, R., & Galindo, J. (2011). Applications of next generation sequencing in molecular
639 ecology of non-model organisms. Heredity, 107(1), 1–15.
640 <https://doi.org/10.1038/hdy.2010.152>

641 Estoup, A., Ravigné, V., Hufbauer, R., Vitalis, R., Gautier, M., & Facon, B. (2016). Is There a
642 Genetic Paradox of Biological Invasion? *Annual Review of Ecology, Evolution, and*
643 *Systematics*, 47, 51–72. <https://doi.org/10.1146/annurev-ecolsys-121415-032116>

644 Facon, B., Pointier, J. P., Jarne, P., Sarda, V., & David, P. (2008). High Genetic Variance in
645 Life-History Strategies within Invasive Populations by Way of Multiple Introductions.
646 *Current Biology*, 18(5), 363–367. <https://doi.org/10.1016/j.cub.2008.01.063>

647 Fitzpatrick, B. M., Fordyce, J. A., Niemiller, M. L., & Reynolds, R. G. (2012). What can DNA
648 tell us about biological invasions? *Biological Invasions*, 14(2), 245–253.
649 <https://doi.org/10.1007/s10530-011-0064-1>

650 Forister, M. L., Dyer, L. A., Singer, M. S., Stireman, J. O., & Lill, J. T. (2012). Revisiting the
651 evolution of ecological specialization, with emphasis on insect-plant interactions.
652 *Ecology*, 93(5), 981–991. <https://doi.org/10.1890/11-0650.1>

653 Fox, E. A., Wright, A. E., Fumagalli, M., & Vieira, F. G. (2019). NgsLD: Evaluating linkage
654 disequilibrium using genotype likelihoods. *Bioinformatics*, 35(19), 3855–3856.
655 <https://doi.org/10.1093/bioinformatics/btz200>

656 Frankham, R. (2005). Resolving the genetic paradox in invasive species. *Heredity*, 94(4), 385.
657 <https://doi.org/10.1038/sj.hdy.6800634>

658 Funk, J. L. (2008). Differences in plasticity between invasive and native plants from a low
659 resource environment. *Journal of Ecology*, 96(6), 1162–1173.
660 <https://doi.org/10.1111/j.1365-2745.2008.01435.x>

661 Futuyma, D. J., & Moreno, G. (1988). The Evolution of Ecological Specialization Author (s):
662 Douglas J . Futuyma and Gabriel Moreno Source : Annual Review of Ecology and
663 Systematics , Vol . 19 (1988), pp . 207-233 Published by : Annual Reviews Stable URL
664 : <http://www.jstor.org/stable/2097>. Annual Review of Ecology and Systematics,
665 19(1988), 207–233.

666 Hardy, O., & Vekemans, X. (2002). Spagedi : a Versatile Computer Program To Analyse
667 Spatial. *Molecular Ecology Notes*, 2, 618–620. <https://doi.org/10.1046/j.1471-8278>

668 Harper, K. E., Bagley, R. K., Thompson, K. L., & Linnen, C. R. (2016). Complementary sex
669 determination, inbreeding depression and inbreeding avoidance in a gregarious sawfly.
670 *Heredity*, 117(5), 326–335. <https://doi.org/10.1038/hdy.2016.46>

671 Hewitt, G. M. (1999). Post-glacial re-colonization of European biota. *Biological Journal of the*
672 *Linnean Society*, 68(1–2), 87–112. <https://doi.org/10.1006/bijl.1999.0332>

673 Hotaling, S., Sproul, J. S., Heckenhauer, J., Powell, A., Larracuente, A. M., Pauls, S. U., Kelley,
674 J. L., & Frandsen, P. B. (2021). Long Reads Are Revolutionizing 20 Years of Insect
675 Genome Sequencing. *Genome Biology and Evolution*, 13(8), 1–7.
676 <https://doi.org/10.1093/gbe/evab138>

677 Jaspers, C., Ehrlich, M., Pujolar, J. M., Kunzel, S., Bayer, T., Limborg, M. T., Lombard, F.,
678 Browne, W. E., Stefanova, K., & Reusch, T. B. H. (2021). Invasion genomics uncover
679 contrasting scenarios of genetic diversity in a widespread marine invader. *Proceedings of*
680 *the National Academy of Sciences of the United States of America*, 118(51).
681 <https://doi.org/10.1073/pnas.2116211118>

682 Jin, W. T., Gernandt, D. S., Wehenkel, C., Xia, X. M., Wei, X. X., & Wang, X. Q. (2021).
683 Phylogenomic and ecological analyses reveal the spatiotemporal evolution of global
684 pines. *Proceedings of the National Academy of Sciences of the United States of America*,
685 118(20). <https://doi.org/10.1073/PNAS.2022302118>

686 Kaňuch, P., Berggren, Å., & Cassel-Lundhagen, A. (2021). A clue to invasion success: genetic
687 diversity quickly rebounds after introduction bottlenecks. *Biological Invasions*, 23(4),
688 1141–1156. <https://doi.org/10.1007/s10530-020-02426-y>

689 Kennedy, G. G., & Storer, N. P. (2000). LIFE SYSTEMS OF POLYPHAGOUS ARTHROPOD
690 PESTS IN TEMPORALLY UNSTABLE CROPPING SYSTEMS. *Annual Review of
691 Entomology*, 45, 467–493.

692 Knerer, A. G., & Atwood, C. E. (2018). Diprionid Sawflies : Polymorphism and Speciation.
693 *Science*, 179(4078), 1090–1099.

694 Kokot, M., Dlugosz, M., & Deorowicz, S. (2017). KMC 3: counting and manipulating k-mer
695 statistics. *Bioinformatics* (Oxford, England), 33(17), 2759–2761.
696 <https://doi.org/10.1093/bioinformatics/btx304>

697 Kolbe, J. J., Glor, R. E., Schettino, L. R. G., Lara, A. C., Larson, A., & Losos, J. B. (2004).
698 Genetic variation increases during a biological invasion. *Nature*, 431(7005), 177–181.

699 Korneliussen, T. S., Albrechtsen, A., & Nielsen, R. (2014). ANGSD: Analysis of Next
700 Generation Sequencing Data. *BMC Bioinformatics*, 15(1), 1–13.
701 <https://doi.org/10.1186/s12859-014-0356-4>

702 Kronenburg, Z., & Sulllivan, S. (2017). Matlock. <https://github.com/phasegenomics/matlock>

703 Lande, R. (2015). Evolution of phenotypic plasticity in colonizing species. *Molecular Ecology*,
704 24(9), 2038–2045. <https://doi.org/10.1111/mec.13037>

705 Langmead, B., & Salzberg, S. L. (2012). Fast gapped-read alignment with Bowtie 2. *Nature
706 Methods*, 9(4), 357–359. <https://doi.org/10.1038/nmeth.1923>

707 Lee, C. E. (2002). Evolutionary genetics of invasive species. *Trends in Ecology and Evolution*,
708 17(8), 386–391. [https://doi.org/10.1016/S0169-5347\(02\)02554-5](https://doi.org/10.1016/S0169-5347(02)02554-5)

709 Lesieur, V., Lombaert, E., Guillemaud, T., Courtial, B., Strong, W., Roques, A., & Auger-
710 Rozenberg, M. A. (2019). The rapid spread of *Leptoglossus occidentalis* in Europe: a
711 bridgehead invasion. *Journal of Pest Science*, 92(1), 189–200.
712 <https://doi.org/10.1007/s10340-018-0993-x>

713 Levy Karin, E., Mirdita, M., & Söding, J. (2020). MetaEuk-sensitive, high-throughput gene
714 discovery, and annotation for large-scale eukaryotic metagenomics. *Microbiome*, 8(1), 1–
715 15. <https://doi.org/10.1186/s40168-020-00808-x>

716 Lewald, K. M., Abrieux, A., Wilson, D. A., Lee, Y., Conner, W. R., Andreazza, F., Beers, E. H.,
717 Burrack, H. J., Daane, K. M., Diepenbrock, L., Drummond, F. A., Fanning, P. D.,
718 Gaffney, M. T., Hesler, S. P., Ioriatti, C., Isaacs, R., Little, B. A., Loeb, G. M., Miller, B.,
719 ... Chiu, J. C. (2021). Population genomics of *Drosophila suzukii* reveal longitudinal
720 population structure and signals of migrations in and out of the continental United States.
721 *G3: Genes, Genomes, Genetics*, 11(12). <https://doi.org/10.1093/g3journal/jkab343>

722 Li, H. (2021). New strategies to improve minimap2 alignment accuracy. *Bioinformatics*, 37(23),
723 4572–4574. <https://doi.org/10.1093/bioinformatics/btab705>

724 Li, H. (2011). A statistical framework for SNP calling, mutation discovery, association mapping
725 and population genetical parameter estimation from sequencing data. *Bioinformatics*,
726 27(21), 2987–2993. <https://doi.org/10.1093/bioinformatics/btr509>

727 Linnen, C. R., & Farrell, B. D. (2010). A test of the sympatric host race formation hypothesis in
728 *Neodiprion* (Hymenoptera: Diprionidae). *Proceedings of the Royal Society B: Biological
729 Sciences*, 277(1697), 3131–3138. <https://doi.org/10.1098/rspb.2010.0577>

730 Looney, C., Smith, D. R., Collman, S. J., Langor, D. W., & Peterson, M. A. (2016). Sawflies
731 (Hymenoptera, Symphyta) newly recorded from Washington State. *Journal of Hymenoptera*

732 Research, 49, 129–159. Lyons, B. (2014). The Use of Classical Biological Control to
733 Preserve Forests in North America: X Introduced Pine Sawfly. In *USDA*.

734 Manni, M., Berkeley, M. R., Seppey, M., Simão, F. A., & Zdobnov, E. M. (2021). BUSCO
735 Update: Novel and Streamlined Workflows along with Broader and Deeper Phylogenetic
736 Coverage for Scoring of Eukaryotic, Prokaryotic, and Viral Genomes. *Molecular Biology*
737 and Evolution

738 Mantel N. (1967). The detection of disease clustering and a generalized regression approach.
739 *Cancer Research*, 27(2), 209–220.

740 Mapleson, D., Accinelli, G. G., Kettleborough, G., Wright, J., & Clavijo, B. J. (2017). KAT: A
741 K-mer analysis toolkit to quality control NGS datasets and genome assemblies.
742 *Bioinformatics*, 33(4), 574–576. <https://doi.org/10.1093/bioinformatics/btw663>

743 McCullough, D. G., & Wagner, M. R. (1993). Defusing host defenses: ovipositional adaptations
744 of sawflies to plant resins. *Sawfly life Hist. Adapt. to woody plants*, 151, 71.

745 Meirmans, P. G. (2012). The trouble with isolation by distance. *Molecular Ecology*, 21(12),
746 2839–2846. <https://doi.org/10.1111/j.1365-294X.2012.05578.x>

747 Meisner, J., & Albrechtsen, A. (2018). Inferring population structure and admixture proportions
748 in low-depth NGS data. *Genetics*, 210(2), 719–731.
<https://doi.org/10.1534/genetics.118.301336>

749 Middleton, W. (1923). *The imported pine sawfly*.

750 North, H. L., McGaughan, A., & Jiggins, C. D. (2021). Insights into invasive species from
751 whole-genome resequencing. *Molecular Ecology*, 30(23), 6289–6308.
<https://doi.org/10.1111/mec.15999>

752 Oerke, E. C. (2006). Crop losses to pests. *Journal of Agricultural Science*, 144(1), 31–43.
<https://doi.org/10.1017/S0021859605005708>

753 Parejo, M., Wragg, D., Henriques, D., Charrière, J. D., & Estonba, A. (2020). Digging into the
754 genomic past of Swiss honey bees by whole-genome sequencing museum specimens.
755 *Genome Biology and Evolution*, 12(12), 2535–2551.
<https://doi.org/10.1093/GBE/EVAA188>

756 Prentis, P. J., Wilson, J. R. U., Dormontt, E. E., Richardson, D. M., & Lowe, A. J. (2008).
757 Adaptive evolution in invasive species. *Trends in Plant Science*, 13(6), 288–294.
<https://doi.org/10.1016/j.tplants.2008.03.004>

758 R Core Team (2021). R: A language and environment for statistical computing. R Foundation for
759 Statistical Computing, Vienna, Austria.

760 Ranallo-Benavidez, T. R., Jaron, K. S., & Schatz, M. C. (2020). GenomeScope 2.0 and
761 Smudgeplot for reference-free profiling of polyploid genomes. *Nature Communications*,
762 11(1). <https://doi.org/10.1038/s41467-020-14998-3>

763 Raxworthy, C. J., & Smith, B. T. (2021). Mining museums for historical DNA: advances and
764 challenges in museomics. *Trends in Ecology and Evolution*, 36(11), 1049–1060.
<https://doi.org/10.1016/j.tree.2021.07.009>

765 Rius, M., & Darling, J. A. (2014). How important is intraspecific genetic admixture to the
766 success of colonising populations? *Trends in Ecology and Evolution*, 29(4), 233–242.
<https://doi.org/10.1016/j.tree.2014.02.003>

767 Roman, J., & Darling, J. A. (2007). Paradox lost: genetic diversity and the success of aquatic
768 invasions. *Trends in Ecology and Evolution*, 22(9), 454–464.
<https://doi.org/10.1016/j.tree.2007.07.002>

777 Rosenthal, D. M., Ramakrishnan, A. P., & Cruzan, M. B. (2008). Evidence for multiple sources
778 of invasion and intraspecific hybridization in *Brachypodium sylvaticum* (Hudson) Beauv.
779 in North America. *Molecular Ecology*, 17(21), 4657–4669.
780 <https://doi.org/10.1111/j.1365-294X.2008.03844.x>

781 Rousselet, J., Géri, C., Hewitt, G. M., & Lemeunier, F. (1998). The chromosomes of *Diprion pini*
782 and *D. similis* (Hymenoptera: Diprionidae): implications for karyotype evolution.
783 *Heredity*, 81(5), 573–578. <https://doi.org/10.1046/j.1365-2540.1998.00421.x>

784 Sakai, A. K., Allendorf, F. W., Holt, J. S., Lodge, D. M., Molofsky, J., With, K. A., Baughman,
785 S., Cabin, R. J., Cohen, J. E., Ellstrand, N. C., Mccauley, D. E., Neil, P. O., Parker, I. M.,
786 Thompson, J. N., & Weller, S. G. (2008). The Population Biology of Invasive Specie
787 Source : Annual Review of Ecology and Systematics , Vol . 32 , (2001), pp . 305-332
788 Published by : Annual Reviews Stable URL : <http://www.jstor.org/stable/2678643>.
789 *Ecology*, 32(2001), 305–332.

790 Sardain, A., Sardain, E., & Leung, B. (2019). Global forecasts of shipping traffic and biological
791 invasions to 2050. *Nature Sustainability*, 2(4), 274–282. <https://doi.org/10.1038/s41893-019-0245-y>

793 Schmidt, T. L., Chung, J., Honnen, A. C., Weeks, A. R., & Hoffmann, A. A. (2020). Population
794 genomics of two invasive mosquitoes (*Aedes aegypti* and *aedes albopictus*) from the
795 indo-pacific. *PLoS Neglected Tropical Diseases*, 14(7), 1–24.
796 <https://doi.org/10.1371/journal.pntd.0008463>

797 Schmidt, T. L., Swan, T., Chung, J., Karl, S., Demok, S., Yang, Q., Field, M. A., Muzari, M. O.,
798 Ehlers, G., Brugh, M., Bellwood, R., Horne, P., Burkot, T. R., Ritchie, S., & Hoffmann,
799 A. A. (2021). Spatial population genomics of a recent mosquito invasion. *Molecular
800 Ecology*, 30(5), 1174–1189. <https://doi.org/10.1111/mec.15792>

801 Scholte, E. J., & Schaffner, F. (2007). Waiting for the tiger: Establishment and spread of the
802 Asian tiger mosquito in Europe. *Emerging Pests and Vector-Borne Diseases in Europe*,
803 14(January 2007), 241–261.

804 Schulz, A. N., Mech, A. M., Allen, C. R., Ayres, M. P., Gandhi, K. J. K., Gurevitch, J., Havill,
805 N. P., Herms, D. A., Hufbauer, R. A., Liebhold, A. M., Raffa, K. F., Raupp, M. J.,
806 Thomas, K. A., Tobin, P. C., & Marsico, T. D. (2020). The impact is in the details:
807 Evaluating a standardized protocol and scale for determining non-native insect impact.
808 *NeoBiota*, 55(August 2019), 61–83. <https://doi.org/10.3897/NEOBIOTA.55.38981>

809 Seebens, H., Essl, F., Dawson, W., Fuentes, N., Moser, D., Pergl, J., Pyšek, P., van Kleunen, M.,
810 Weber, E., Winter, M., & Blasius, B. (2015). Global trade will accelerate plant invasions
811 in emerging economies under climate change. *Global Change Biology*, 21(11), 4128–
812 4140. <https://doi.org/10.1111/gcb.13021>

813 Seeman, T. (2018). any2fasta (0.4.2). <https://github.com/tseemann/any2fasta>

814 Sherpa, S., Blum, M. G. B., Capblancq, T., Cumer, T., Rioux, D., & Després, L. (2019).
815 Unravelling the invasion history of the Asian tiger mosquito in Europe. *Molecular
816 Ecology*, 28(9), 2360–2377. <https://doi.org/10.1111/mec.15071>

817 Sherpa, S., Rioux, D., Pougnet-Lagarde, C., & Després, L. (2018). Genetic diversity and
818 distribution differ between long-established and recently introduced populations in the
819 invasive mosquito *Aedes albopictus*. *Infection, Genetics and Evolution*, 58(December
820 2017), 145–156. <https://doi.org/10.1016/j.meegid.2017.12.018>

821 Shriner, D. (2011). Investigating population stratification and admixture using eigenanalysis of
822 dense genotypes. *Heredity*, 107(5), 413–420. <https://doi.org/10.1038/hdy.2011.26>

823 Sim, S. B. (2022). blobblurb. <https://github.com/sheinasim/blobblurb>

824 Sim, S. B., Corpuz, R. L., Simmonds, T. J., & Geib, S. M. (2022). HiFiAdapterFilt, a memory
825 efficient read processing pipeline, prevents occurrence of adapter sequence in PacBio
826 HiFi reads and their negative impacts on genome assembly. *BMC Genomics*, 23(1), 1–7.
827 <https://doi.org/10.1186/s12864-022-08375-1>

828 Simberloff, D., Martin, J. L., Genovesi, P., Maris, V., Wardle, D. A., Aronson, J., Courchamp,
829 F., Galil, B., García-Berthou, E., Pascal, M., Pyšek, P., Sousa, R., Tabacchi, E., & Vilà,
830 M. (2013). Impacts of biological invasions: What's what and the way forward. *TRENDS
831 in Ecology and Evolution*, 28(1), 58–66. <https://doi.org/10.1016/j.tree.2012.07.013>

832 Skotte, L., Korneliussen, T. S., & Albrechtsen, A. (2013). Estimating individual admixture
833 proportions from next generation sequencing data. *Genetics*, 195(3), 693–702.
834 <https://doi.org/10.1534/genetics.113.154138>

835 Stanke, M., Diekhans, M., Baertsch, R., & Haussler, D. (2008). Using native and syntenically
836 mapped cDNA alignments to improve de novo gene finding. *Bioinformatics*, 24(5), 637–
837 644. <https://doi.org/10.1093/bioinformatics/btn013>

838 van Boheemen, L. A., Lombaert, E., Nurkowski, K. A., Gauffre, B., Rieseberg, L. H., &
839 Hodgins, K. A. (2017). Multiple introductions, admixture and bridgehead invasion
840 characterize the introduction history of *Ambrosia artemisiifolia* in Europe and Australia.
841 *Molecular Ecology*, 26(20), 5421–5434. <https://doi.org/10.1111/mec.14293>

842 Van Petegem, K., Moerman, F., Dahirel, M., Fronhofer, E. A., Vandegehuchte, M. L., Van
843 Leeuwen, T., Wybouw, N., Stoks, R., & Bonte, D. (2018). Kin competition accelerates
844 experimental range expansion in an arthropod herbivore. *Ecology Letters*, 21(2), 225–
845 234. <https://doi.org/10.1111/ele.12887>

846 Vertacnik, K. L., & Linnen, C. R. (2017). Evolutionary genetics of host shifts in herbivorous
847 insects: insights from the age of genomics. *Annals of the New York Academy of
848 Sciences*, 1389(1), 186–212. <https://doi.org/10.1111/nyas.13311>

849 Wonham, M. J., Walton, W. C., Ruiz, G. M., Frese, A. M., & Galil, B. S. (2001). Going to the
850 source: Role of the invasion pathway in determining potential invaders. *Marine Ecology
851 Progress Series*, 215, 1–12. <https://doi.org/10.3354/meps215001>

852 Yoshida, T., Goka, K., Ishihama, F., Ishihara, M., & Kudo, S. I. (2007). Biological invasion as a
853 natural experiment of the evolutionary processes: Introduction of the special feature.
854 *Ecological Research*, 22(6), 849–854. <https://doi.org/10.1007/s11284-007-0435-3>

855 Zappe, M. P. (1917). Egg-Laying Habits of *Diprion Simile* Hartig. *Journal of Economic
856 Entomology*, 10(1), 188–190. <https://doi.org/10.1093/jee/10.1.188>

857 Zenni, R. D., Lamy, J. B., Lamarque, L. J., & Porté, A. J. (2014). Adaptive evolution and
858 phenotypic plasticity during naturalization and spread of invasive species: Implications
859 for tree invasion biology. *Biological Invasions*, 16(3), 635–644.
860 <https://doi.org/10.1007/s10530-013-0607-8>